

哈爾濱工程大學  
HARBIN ENGINEERING UNIVERSITY

INPC 2025, Daejeon

# Further test of applying the envelope method to the optical potential ambiguity problem

Liyuan Hu (胡力元)

College of Nuclear Science and Technology, Harbin Engineering University

2025. 05



01 Introduction

02 Methods

03 Results and Analyses

04 Conclusions

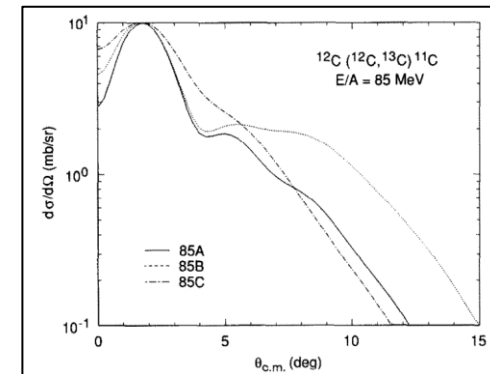
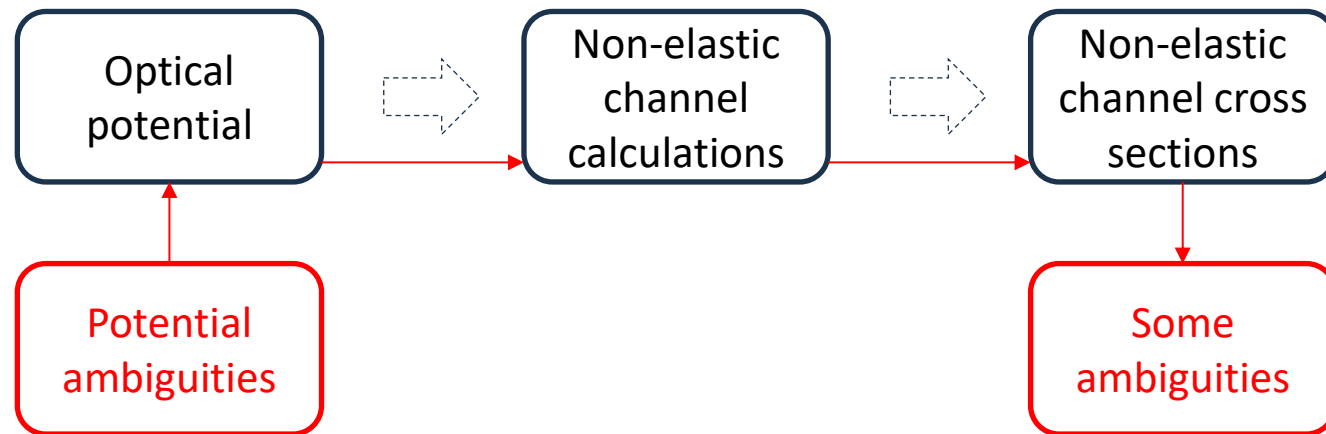
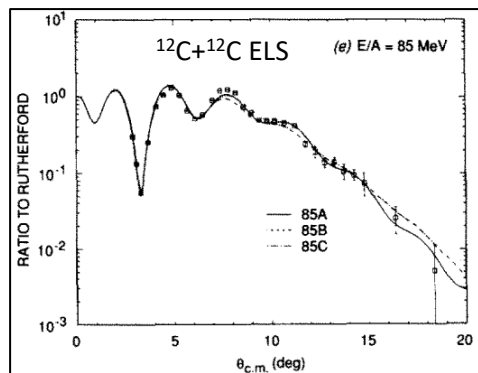


# 01 Introduction

## 1. What is the **optical potential ambiguity problem**?

For a specific data set of the elastic scattering angular distribution, different optical potential sets can provide nearly equivalent agreement.

- Continuous ambiguity
- Discrete ambiguity in the real part
- Shallow- or deep- $W$  ambiguity



# 01 Introduction



## 2. What is the envelope method?

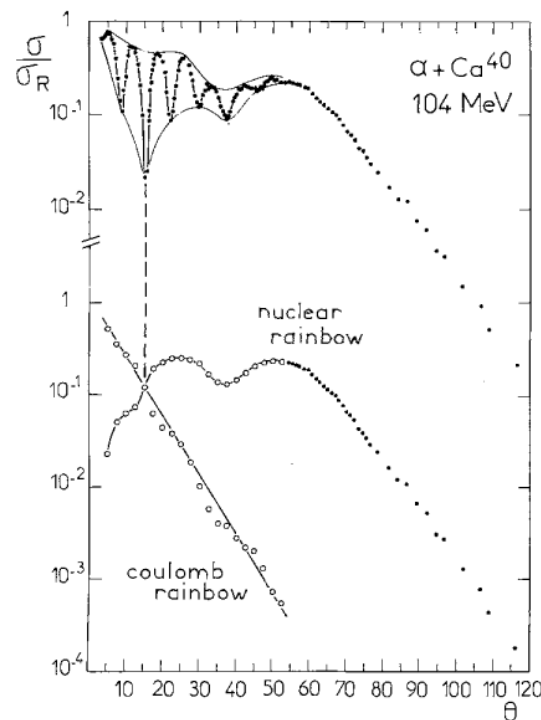
$$f(\theta) = |f_-(\theta)| e^{i\alpha_-(\theta)} + |f_+(\theta)| e^{i\alpha_+(\theta)} \quad (4)$$

where  $|f_-(\theta)|^2 = \sigma_-(\theta)$  and  $|f_+(\theta)|^2 = \sigma_+(\theta)$  are interpreted [7] as being the differential cross sections for scattering through “positive” and “negative angles”, respectively. The  $\sigma_{\pm}(\theta)$  as well as the phases  $\alpha_{\pm}(\theta)$ , can be evaluated either by solving numerically the Schrödinger equation or by approximate methods: stationary phase approximation [7], uniform approximation [8], etc.

Taking the square modulus of (4), one immediately recognizes that  $|f(\theta)|^2 = d\sigma/d\Omega$ , will oscillate between the two limits  $E_+$  and  $E_-$  defined by,

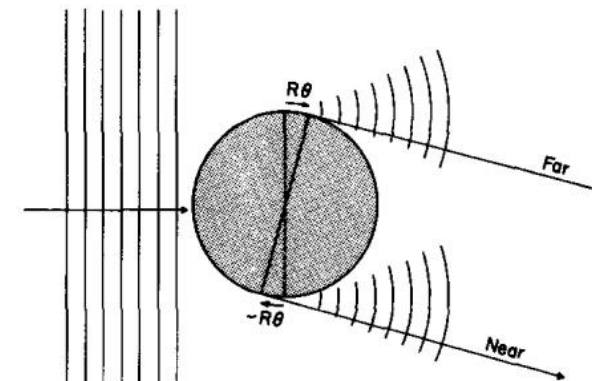
$$\begin{aligned} E_+(\theta) &= (\sigma_-(\theta)^{1/2} + \sigma_+(\theta)^{1/2})^2, \\ E_-(\theta) &= (\sigma_-(\theta)^{1/2} - \sigma_+(\theta)^{1/2})^2 \end{aligned} \quad (5)$$

These limits define the envelopes of the oscillatory pattern of the scattering cross-section. Such envelopes are easy to draw every time the extrema of the oscillatory pattern are well defined in the experimental data. If so, it becomes straightforward to obtain  $\sigma_-(\theta)$  and  $\sigma_+(\theta)$  at each scattering angle.



R. da Silva, Ch. Leclercq-Willain. On the separation of the nuclear and Coulomb rainbow components from the elastic scattering data. Z. Phys. A, 314, 63-67 (1983).

Farside: negative deflection angle



Nearside: positive deflection angle

M.S. Hussein, K.W. McVoy. Nearside and farside: The optics of heavy ion elastic scattering. Prog. Part. Nucl. Phys., 12, 103-170 (1984).

# 01 Introduction

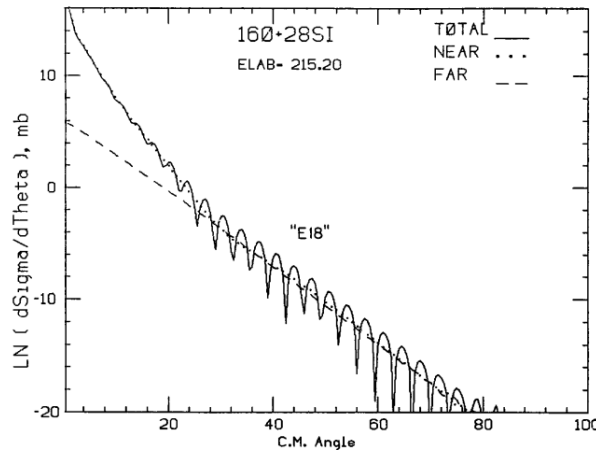
## 3. What is the link between the optical potential ambiguity problem and the envelope method?

Ambiguous refractive and diffractive potentials show evidently **different nearside and farside behaviors at high energies**.

- Refractive potential ( $V \gg W$ , but  $R_V < R_W$ ; Fraunhofer crossover): nearside shows a larger slope than the farside.
- Diffractive potential ( $V < W$ ; no crossover and a wider Fraunhofer oscillations): nearside and farside are nearly parallel.

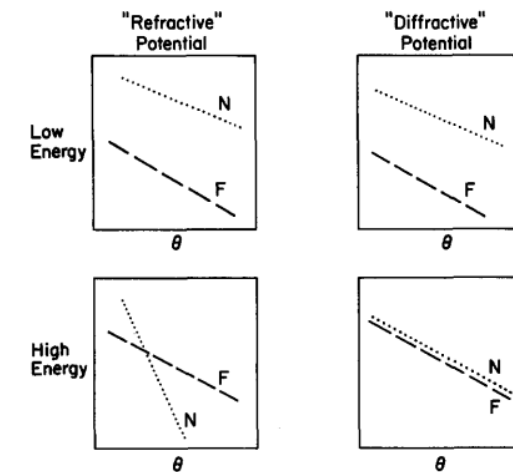
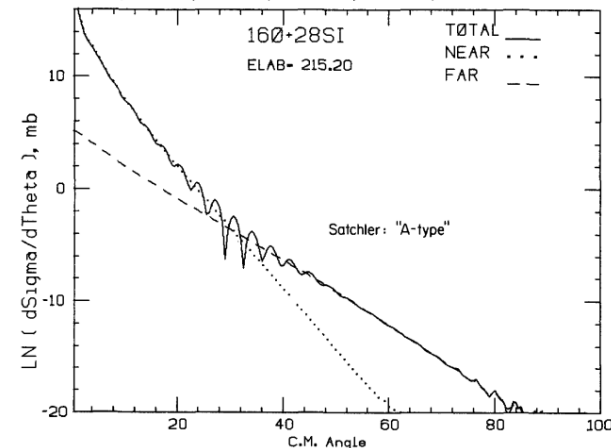
Diffractive shallow-V "E18"

1/4-THETA= 9.9, K=AI= 4.51, THETA(NR)=177. AT L(NR)=200  
V= 10.00, R= 7.50, A=0.618, VI= 23.40, RI= 6.83, AI=0.552



Refractive deep-V "A-type"

1/4-THETA=11.3, K=AI= 6.94, THETA(NR)=177. AT L(NR)=200  
V=100.00, R= 5.37, A=0.745, VI= 44.10, RI= 5.96, AI=0.850

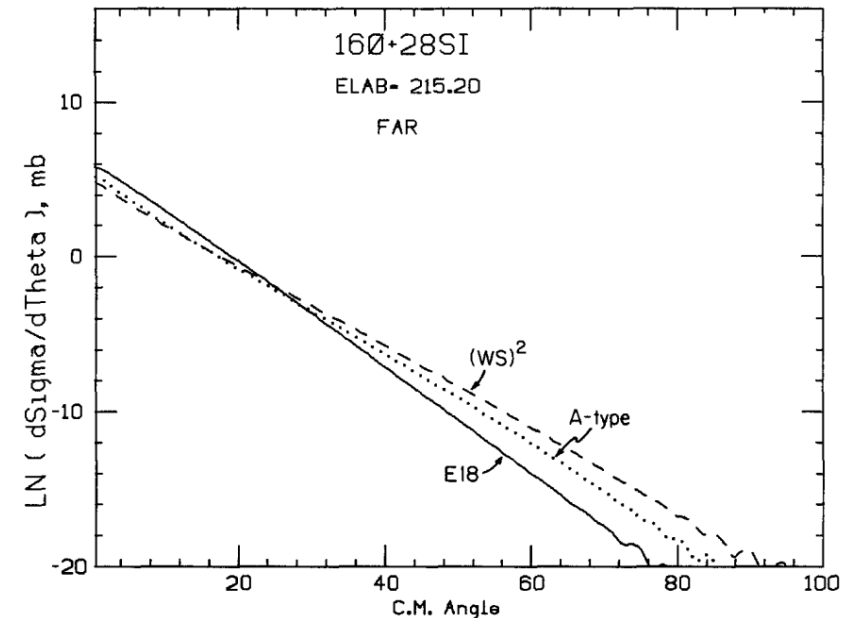
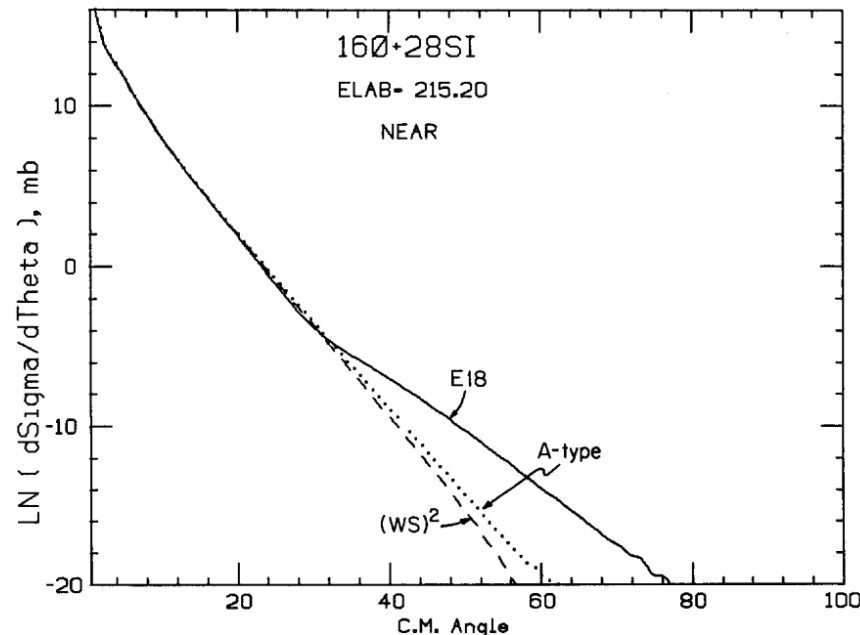


# 01 Introduction



### 3. What is the link between the optical potential ambiguity problem and the envelope method?

The nearside components for the refractive and diffractive potentials show different slopes.  
So does the farside one.



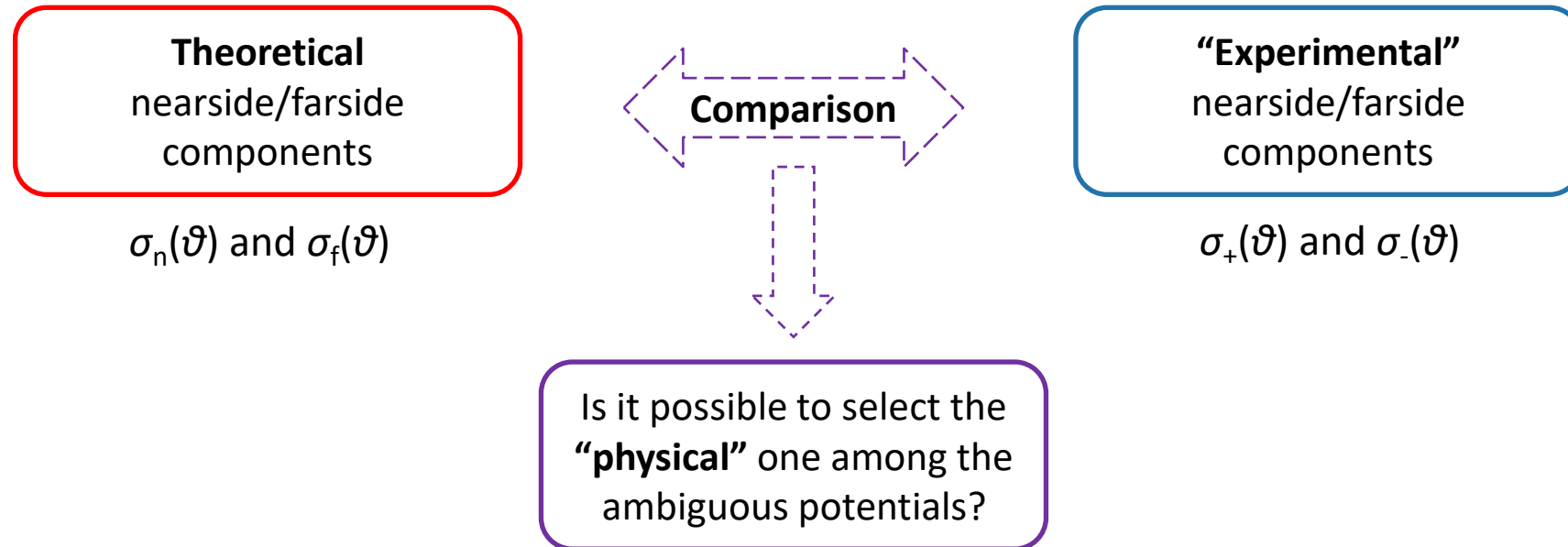
# 01 Introduction



3. What is the link between the optical potential ambiguity problem and the envelope method?

## INSPIRATION

Is it possible to deal with the optical potential ambiguity problem by using the envelope method?



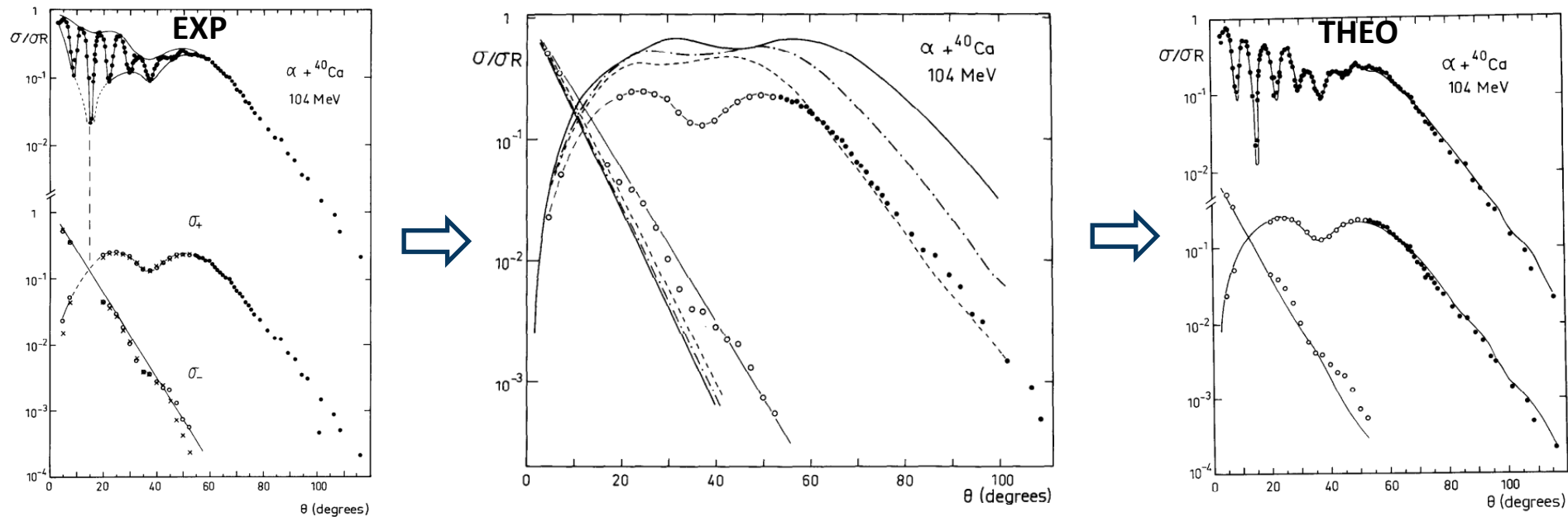


# 01 Introduction



### 3. What is the link between the optical potential ambiguity problem and the envelope method?

A pioneering work used this comparison to determine the  $\alpha$ -nucleus interaction and found that the comparison with respect to the farside component is more sensitive to the imaginary potential than elastic scattering.





## 4. What we have done

- Add some **range estimation** of the “experimental” nearside/farside components in the envelope method.
- As the starting point, test the envelope method to the **refractive/surface-transparent (including refractive/diffractive)** potential ambiguity.
- Further, test the envelope method to the **shallow-/deep- $W$**  potential ambiguity.
- Summarize the **factors influencing the application** of the envelope method to the potential ambiguity.

# 02 Methods



## 1. The envelope method

### Scattering amplitudes

(+—positive deflection angle, —negative deflection angle)

(The sign is opposite to the original work, but same to Lassaut's work)

$$f(\theta) = f_+(\theta) + f_-(\theta)$$

### Cross sections

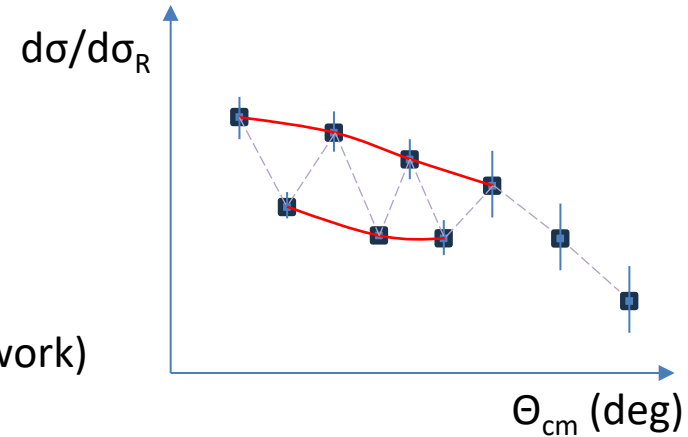
$$\sigma_{\pm}(\theta) = |f_{\pm}(\theta)|^2$$

### Envelopes

(u—upper, l—lower)

$$E_u(\theta) = \left( \sigma_+^{1/2}(\theta) + \sigma_-^{1/2}(\theta) \right)^2$$

$$E_l(\theta) = \left( \sigma_+^{1/2}(\theta) - \sigma_-^{1/2}(\theta) \right)^2$$



- **Envelopes determination**

- The upper and lower envelopes were drawn by connecting these maxima and minima with broken lines, respectively.
- The broken lines were then smoothed using the TGraph class provided by the **CERN ROOT software**.

*L.Y. Hu, Y.S. Song. Trial application of the envelope method to the potential ambiguity problem. Nucl. Sci. Tech., 35, 8 (2024).*

# 02 Methods



## 1. The envelope method

### Scattering amplitudes

(+—positive deflection angle, —negative deflection angle)

(The sign is opposite to the original work, but same to Lassaut' s work)

$$f(\theta) = f_+(\theta) + f_-(\theta)$$

### Cross sections

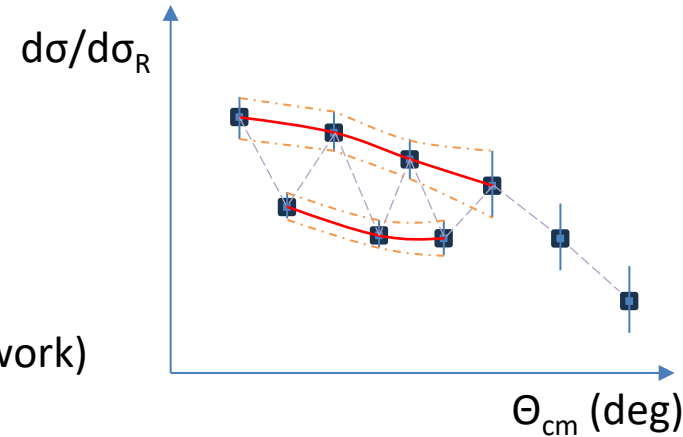
$$\sigma_{\pm}(\theta) = |f_{\pm}(\theta)|^2$$

### Envelopes

(u—upper, l—lower)

$$E_u(\theta) = \left( \sigma_+^{1/2}(\theta) + \sigma_-^{1/2}(\theta) \right)^2$$

$$E_l(\theta) = \left( \sigma_+^{1/2}(\theta) - \sigma_-^{1/2}(\theta) \right)^2$$



- **Add range estimation to the original envelope method**
  - The envelopes were drawn for  $\mu + dev$ ,  $\mu$  and  $\mu - dev$ , where  $\mu$  and  $dev$  are the mean values and the standard deviation of **the experimental data points**, respectively.
  - The **mean values of  $\sigma_{\pm}(\vartheta)$**  were obtained by combining the upper and lower  **$\mu$  envelopes**. The other combinations of upper and lower envelopes were used **to limit  $\sigma_+(\vartheta)$  and  $\sigma_-(\vartheta)$** .

*L.Y. Hu, Y.S. Song. Trial application of the envelope method to the potential ambiguity problem. Nucl. Sci. Tech., 35, 8 (2024).*

## 2. The theoretical nearside/farside decomposition

Scattering amplitudes

(n—nearside, f—farside)

$$f(\theta) = f_n(\theta) + f_f(\theta) \quad \leftarrow \quad f_{n/f}(\theta) = \frac{1}{2ik} \sum_{n=1}^{\infty} (2l+1) [e^{2i\delta_l} - e^{2i\sigma_l}] Q_l^{(\mp)}(\cos\theta) + f_{C,n/f}(\theta)$$

Cross sections

$$\sigma_{n/f}(\theta) = |f_{n/f}(\theta)|^2$$

## 3. Comparison to select the more “physical” potential among the ambiguous potentials

$$\sigma_n(\theta) \quad \text{vs} \quad \sigma_+(\theta)$$

$$\sigma_f(\theta) \quad \text{vs} \quad \sigma_-(\theta)$$

- **Optical model calculations** (including **optical potential** and **phase shift determination**)
  - FRESKO code [I.J. Thompson, *Coupled reaction channels calculations in nuclear physics. Comput. Phys. Rep.* 7, 167–212 (1988).]
- **Nearside/farside decomposition**
  - Theoretical method: R.C. Fuller. *Qualitative behavior of heavy-ion elastic scattering angular distributions. Phys. Rev. C* 12, 1561–1574 (1975).
  - Numerical algorithm: M.H. Cha. *NearFar: a computer program for nearside-farside decomposition of heavy-ion elastic scattering amplitude. Comput. Phys. Commun.* 176, 318–325 (2007).

# 03 Results and Analyses

1. In the previous work, we have revisited the “refractive/surface-transparent” potential ambiguity by using the envelope method.

$^{16}\text{O} + ^{28}\text{Si}$  at 215.2 MeV

□ In this case, the comparison cannot be used to select the “physical” potential.

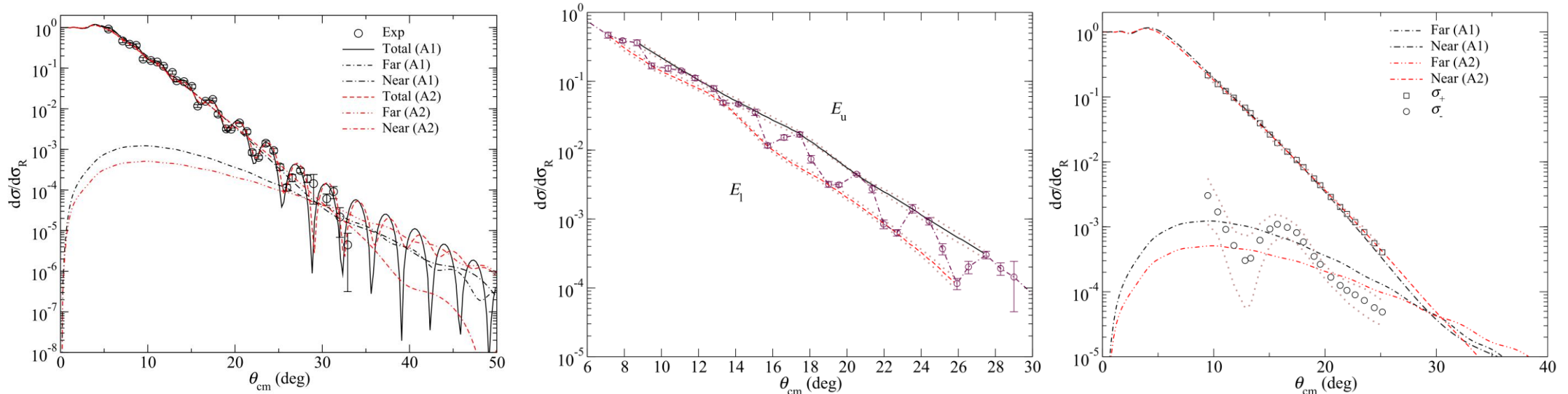
| Colliding system                 | Potential set | $V_0$ (MeV) | $r_R$ (fm) | $a_R$ (fm) | $W_0$ (MeV) | $r_I$ (fm) | $a_I$ (fm) |
|----------------------------------|---------------|-------------|------------|------------|-------------|------------|------------|
| $^{16}\text{O} + ^{28}\text{Si}$ | A1            | 10.00       | 1.350      | 0.618      | 23.40       | 1.230      | 0.552      |
|                                  | A2            | 100.00      | 0.967      | 0.745      | 44.10       | 1.073      | 0.850      |

[Note]

Potentials are from G.R. Satchler. Nucl. Phys. A 279, 493–501 (1977).

surface transparent

refractive



L.Y. Hu, Y.S. Song. Trial application of the envelope method to the potential ambiguity problem. Nucl. Sci. Tech., 35, 8 (2024).

# 03 Results and Analyses



1. In the previous work, we have revisited the “refractive/surface-transparent” potential ambiguity by using the envelope method.

$^{12}\text{C} + ^{12}\text{C}$  at 1016 MeV

□ In this case, the comparison has selected the refractive potential as the “physical” one.

| Colliding system              | Potential set | $V_0$ (MeV) | $r_R$ (fm) | $a_R$ (fm) | $W_0$ (MeV) | $r_I$ (fm) | $a_I$ (fm) |
|-------------------------------|---------------|-------------|------------|------------|-------------|------------|------------|
| $^{12}\text{C}+^{12}\text{C}$ | B1            | 49.90       | 0.934      | 0.742      | 150.40      | 0.262      | 1.201      |
|                               | B2            | 129.4       | 0.681      | 0.913      | 47.90       | 0.918      | 0.622      |

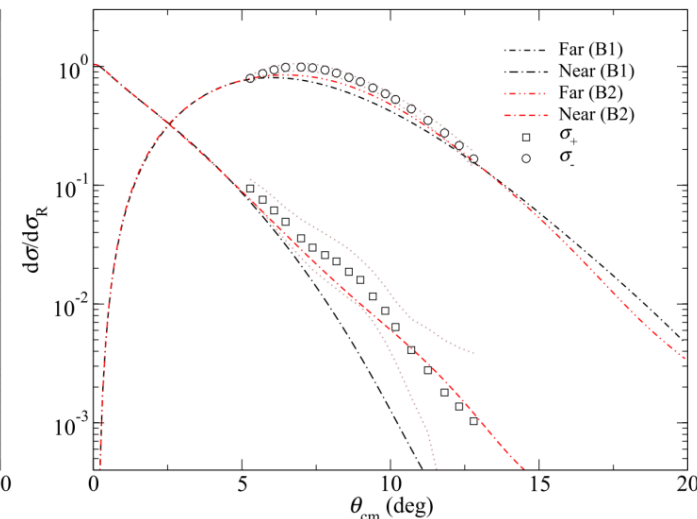
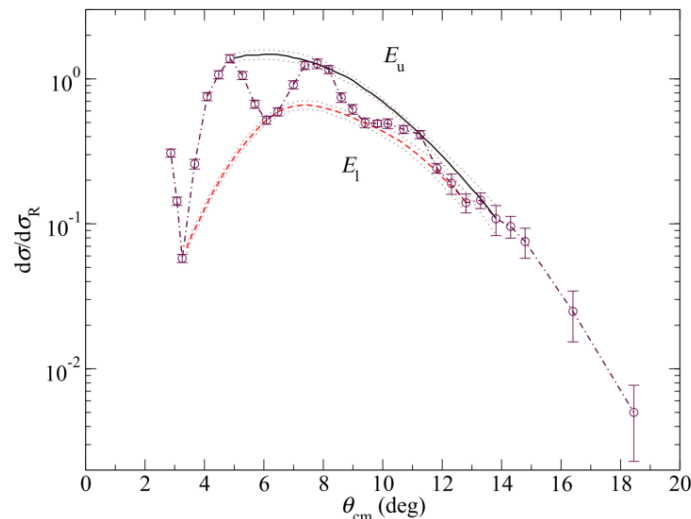
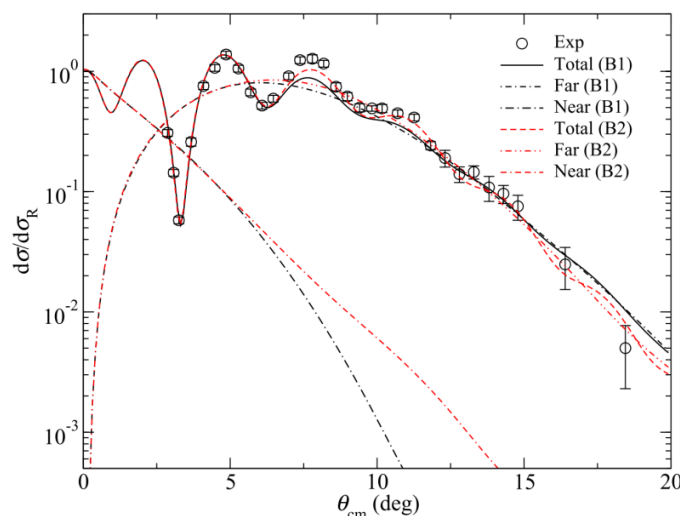
[Note]

Potentials are from G.R. Satchler. Nucl. Phys. A, 505, 103-122 (1989).

surface transparent

It is indeed the shallow-/deep-  
W ambiguity.

refractive



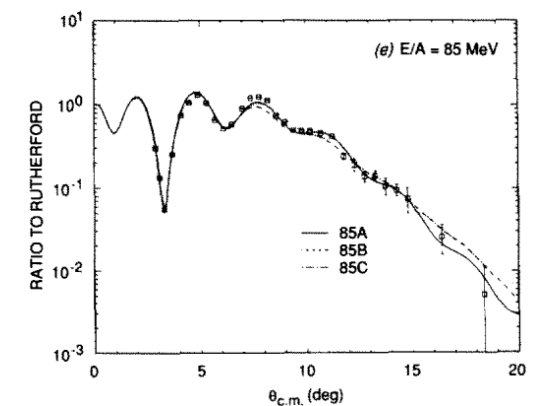
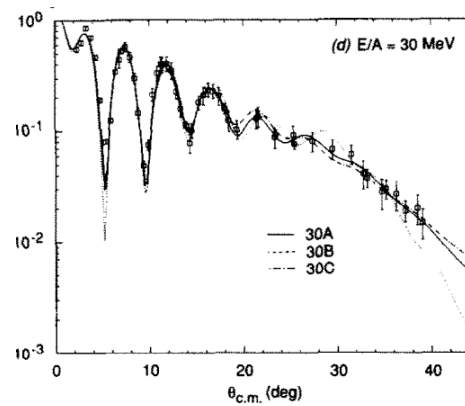
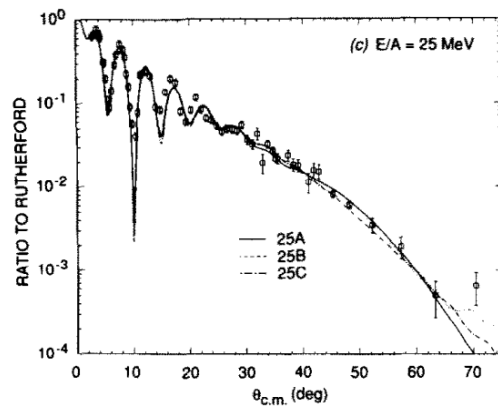
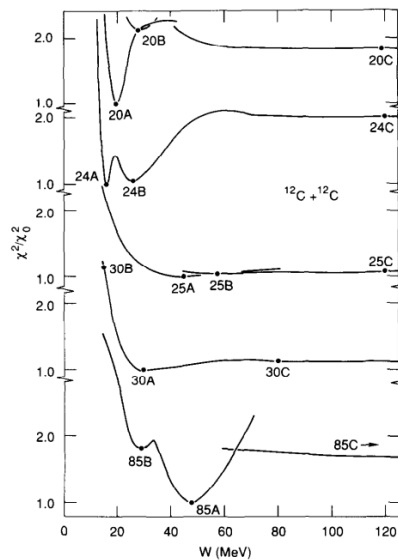
# 03 Results and Analyses



2. In the present work, we have further tested the envelope method for the shallow-/deep- $W$  potential ambiguity.

At the same time, this analysis indicated that some of the data sets (such as  $^{16}\text{O} + ^{12}\text{C}$  at 608 MeV in Fig. 7.6) could be described well by potentials with either a shallow or a deep imaginary part. It is the continuity requirement between different energies that led the authors in [27] and [28] to choose the weakly absorptive solution as the “correct” one; later studies showed that in some cases the best fit (in terms of giving the minimum  $\chi^2$ ) might actually correspond to the potential with the stronger absorption, indicating that the  $\chi^2$  criterion should be treated with caution.

M.E. Brandan, G.R. Satchler. *The interaction between light heavy-ions and what it tells us. Phys. Rep., 285, 143-243 (1997).*



G.R. Satchler. *Transfer reactions and optical potential ambiguities for light heavy-ion systems. Nucl. Phys. A, 505, 103-122 (1989).*



# 03 Results and Analyses



2. In the present work, we have further tested the envelope method for the shallow-/deep-W potential ambiguity.

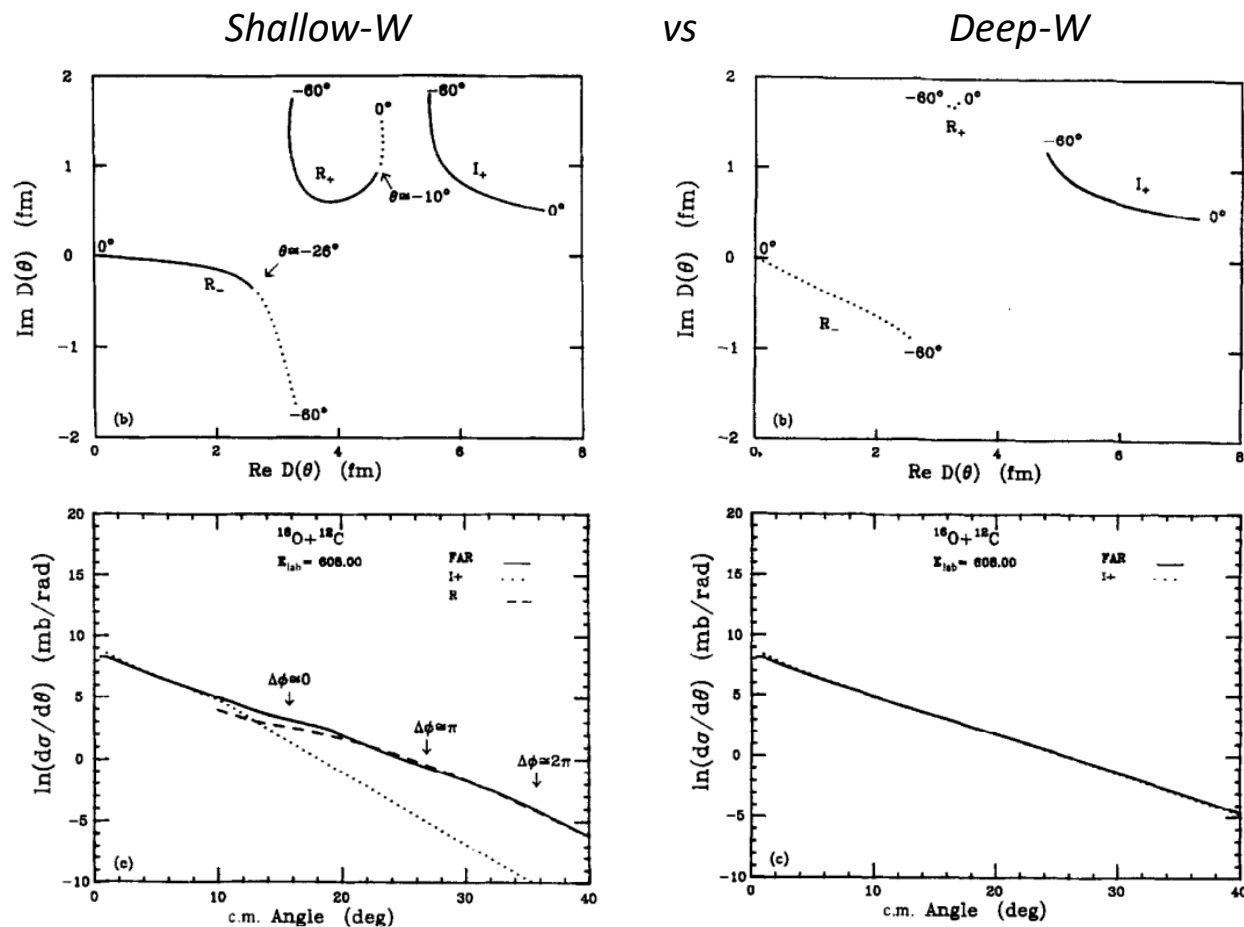
$^{16}\text{O} + ^{12}\text{C}$  at 608 MeV

- The physical explanation of shallow-/deep-W potential ambiguity
  - In the deep-W potential case, the edge diffractive trajectory ( $I_+$ ) is capable of producing a **farside** amplitude similar to that produced by the weak-W potential, in which case the farside amplitude is composed of refractive ( $R_+$ ,  $R_-$ ) and diffractive ( $I_+$ ) trajectories both.

*S.H. Fricke, et al. Phys. Rev. C, 38, 682-695 (1988).*

*M.E. Brandan, G.R. Satchler. Phys. Rep., 285, 143-243 (1997).*

- However, how about the nearside behavior?



# 03 Results and Analyses



2. In the present work, we have further tested the envelope method for the shallow-/deep- $W$  potential ambiguity.

$^{16}\text{O} + ^{12}\text{C}$  at 608 MeV

- **OM calculations and potential determined**

- **Woods-Saxon** shape for both real and imaginary part of the optical potential
- For the **shallow- $W$  potential**, the unambiguous potential proposed by Brandan was adopted ( $W_0=24.7$  MeV).

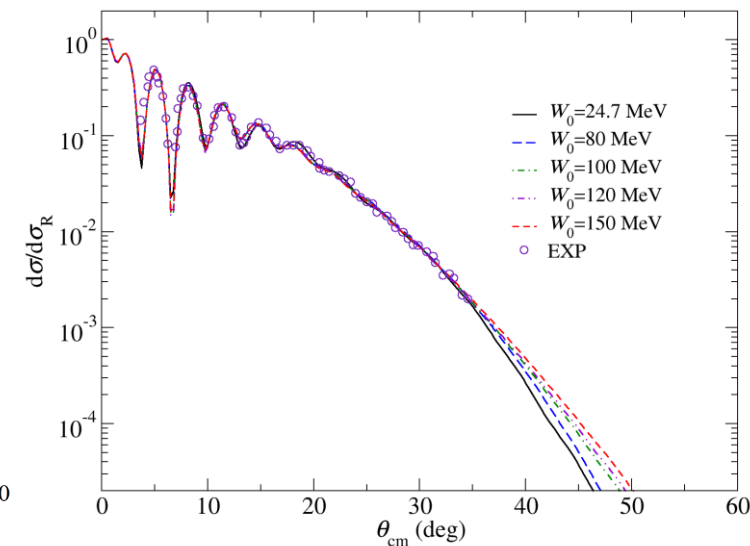
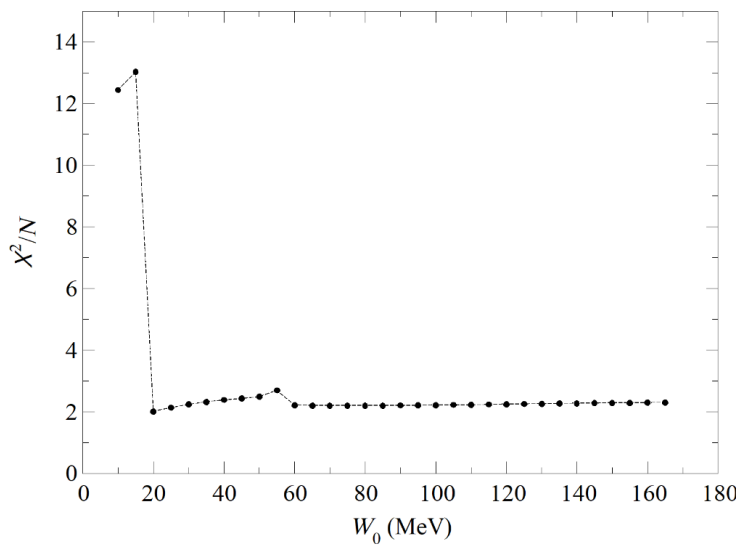
*M.E. Brandan. Phys. Rev. Lett., 60, 784-787 (1988).*

- For the **deep- $W$  potential**,  $W_0=80, 100, 120$  and  $150$  MeV were selected.

====>

- ▣ The experimental data are reproduced equally well.

$$\chi^2 = \sum_{i=1}^N \left[ \frac{\sigma_{\text{theor}}(\theta_i) - \sigma_{\text{expt}}(\theta_i)}{\Delta\sigma_{\text{expt}}(\theta_i)} \right]^2$$



*A uniform error of 10% was assumed in the data fitting*

# 03 Results and Analyses



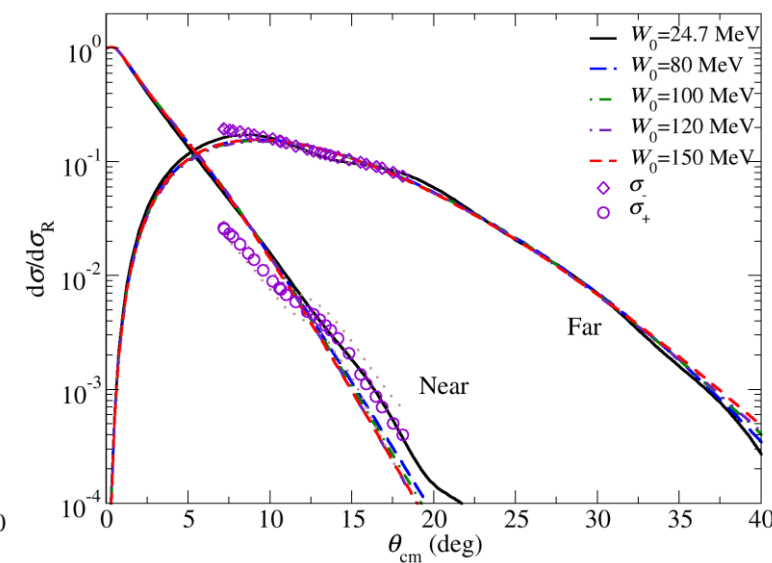
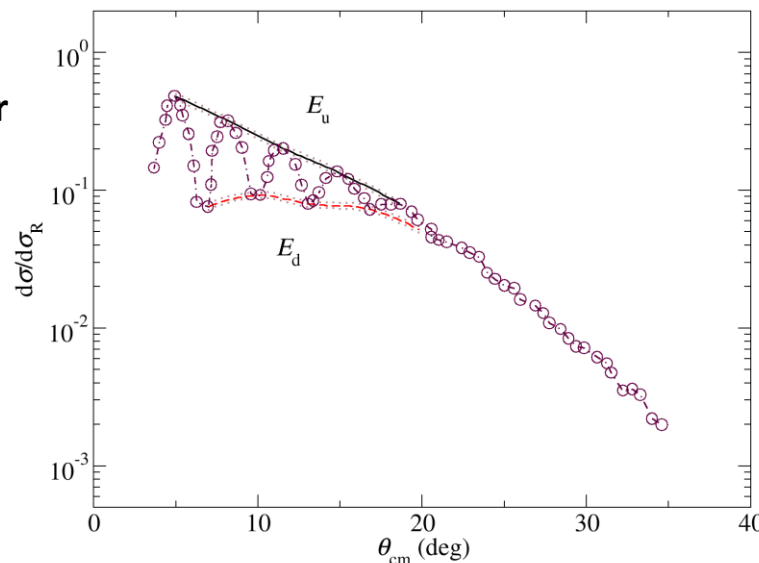
2. In the present work, we have further tested the envelope method for the shallow-/deep- $W$  potential ambiguity.

$^{16}\text{O} + ^{12}\text{C}$  at 608 MeV

- Envelope method and N/F comparison

==>

- The five potential sets produce very **similar farside** components.
- The four deep- $W$  potential sets show **concentrated feature** in the **nearside**.
- Deep- $W$  potential sets show evident distinction with the shallow- $W$  one in the **nearside**.
- $\sigma_-(\vartheta)$  and  $\sigma_f(\vartheta)$  match well.
- $\sigma_+(\vartheta)$  matches the  $\sigma_n(\vartheta)$  corresponding to shallow- $W$  potential well within the limitations.



*A uniform error of 10% was assumed in the envelope plot*

# 03 Results and Analyses

2. In the present work, we have further tested the envelope method for the shallow-/deep- $W$  potential ambiguity.

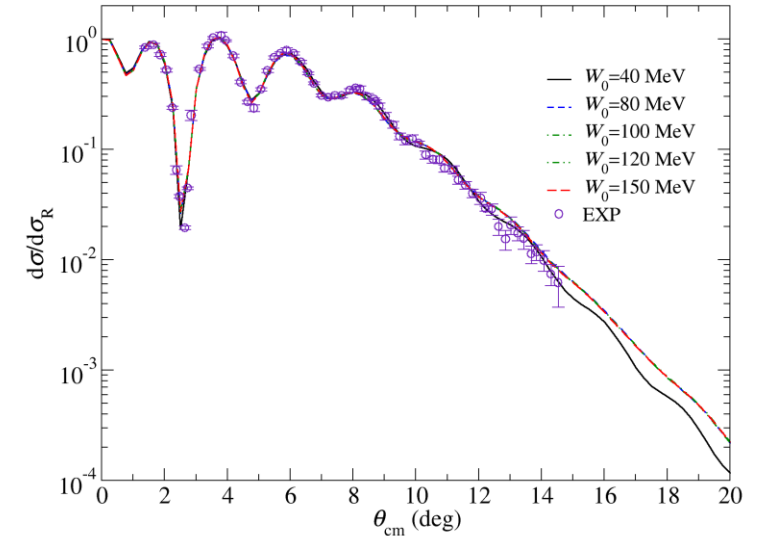
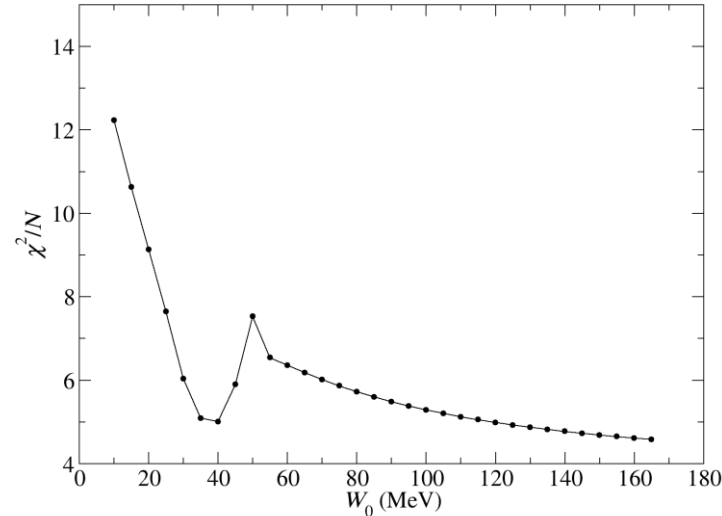
$^{16}\text{O} + ^{12}\text{C}$  at 1503 MeV

$$\chi^2 = \sum_{i=1}^N \left[ \frac{\sigma_{\text{theor}}(\theta_i) - \sigma_{\text{expt}}(\theta_i)}{\Delta\sigma_{\text{expt}}(\theta_i)} \right]^2$$

- **OM calculations and potential determined**
  - For the **shallow- $W$**  potential, the discrete family with  $W_0=40$  MeV was utilized.
  - For the **deep- $W$**  potential,  $W_0=80, 100, 120$  and 150 MeV were selected.

==>

- The experimental data are reproduced equally well.



*A uniform error of 10% was assumed in the data fitting.*

# 03 Results and Analyses

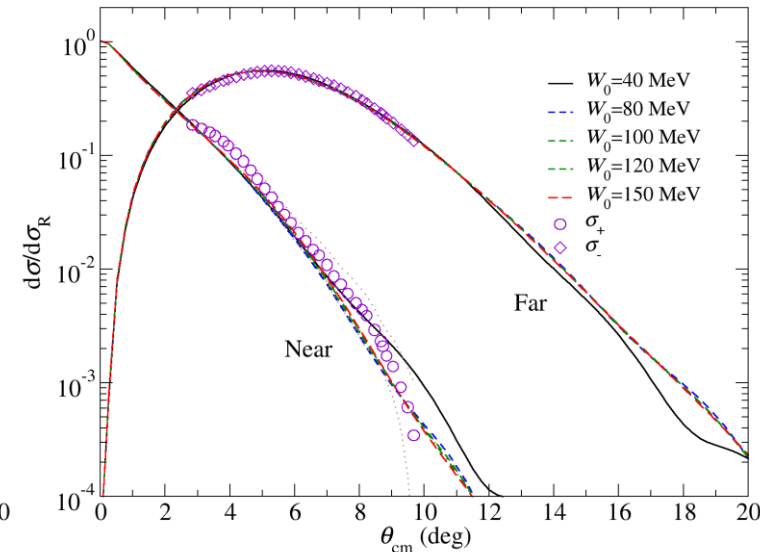
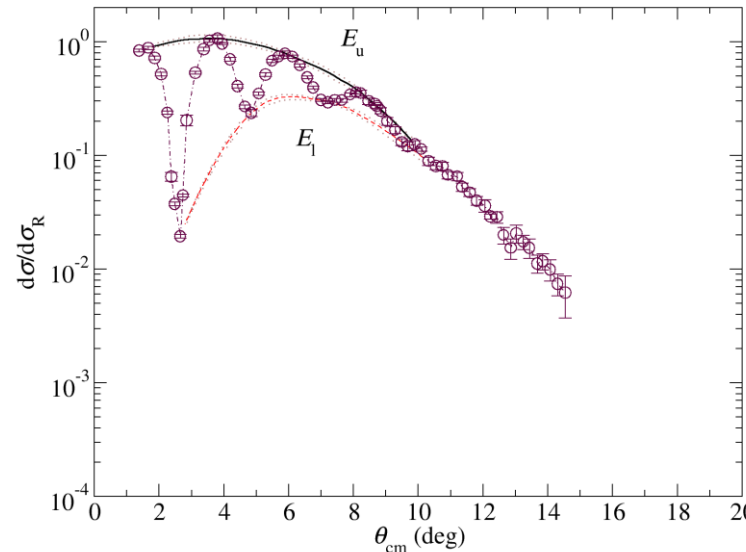
2. In the present work, we have further tested the envelope method for the shallow-/deep- $W$  potential ambiguity.

$^{16}\text{O} + ^{12}\text{C}$  at 1503 MeV

- Envelope method and N/F comparison

===>

- ❑ The five potential sets produce very **similar farside** components.
- ❑ The four deep- $W$  potential sets show **concentrated feature** in the **nearside**.
- ❑ Deep- $W$  potential sets show evident distinction with the shallow- $W$  one in the **nearside**.
- ❑  $\sigma_-(\vartheta)$  and  $\sigma_f(\vartheta)$  match well.
- ❑  $\sigma_+(\vartheta)$  matches the  $\sigma_n(\vartheta)$  corresponding to shallow- $W$  potential well within the limitations.
- ❑ When the  $\sigma_+(\vartheta)$  falls below  $\sim 10^{-3}$ , the comparison become less meaningful.



The experimental error was assumed in the envelope plot.

# 04 Conclusions

1. The envelope method shows its capability of dealing with **the shallow-/deep- $W$  potential ambiguity problem**.
2. Before, we have summarized the **factors influencing the applications of the envelope method**, which are also suitable for its application to shallow-/deep- $W$  potential ambiguity problem.
  - The difference between the calculated  $\sigma_{n/f}$  corresponding to different potential families  $\rightarrow$  **evident**
  - The magnitude of the smaller parts of  $\sigma_{\pm} \rightarrow >\sim 10^{-3}$
  - The data quality  $\rightarrow$  **small angular resolution and statistical error**
  - The Fraunhofer crossover  $\rightarrow$  **not too close to it**

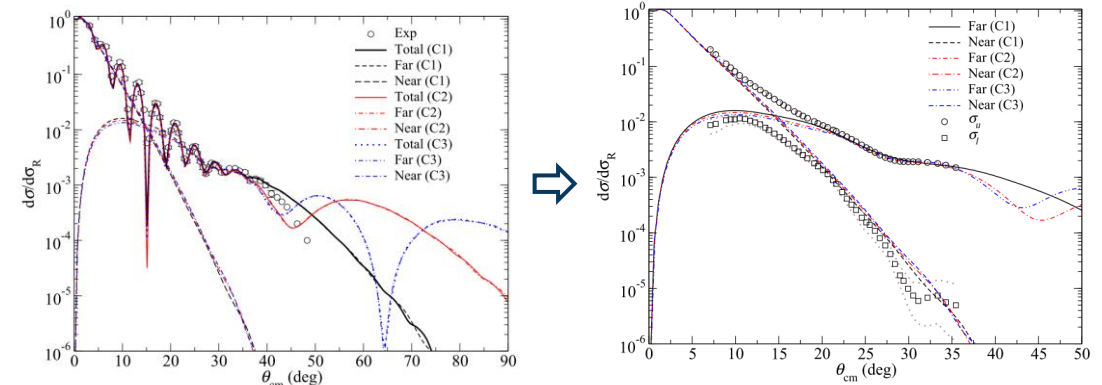
| colliding<br>system                | potential<br>set | $V_0$<br>(MeV) | $r_R$<br>(fm) | $a_R$<br>(fm) | $W_0$<br>(MeV) | $r_I$<br>(fm) | $a_I$<br>(fm) |
|------------------------------------|------------------|----------------|---------------|---------------|----------------|---------------|---------------|
| ${}^6\text{Li} + {}^{58}\text{Ni}$ | C1               | 173.66         | 0.770         | 0.903         | 32.27          | 1.080         | 0.817         |
|                                    | C2               | 266.38         | 0.694         | 0.906         | 32.94          | 1.080         | 0.818         |
|                                    | C3               | 359.63         | 0.653         | 0.887         | 34.47          | 1.070         | 0.831         |

[Note]

Potentials are from M.E. Brandan and K.W. McVoy. *Phys. Rev. C*, 43, 1140 (1991).

- Due to the too close N/F components among discrete- $V$  families, it seems not hopeful to use envelope method to select potential from the discretely ambiguous ones.

${}^6\text{Li} + {}^{58}\text{Ni}$  at 210 MeV  
 discrete- $V$  potential ambiguity

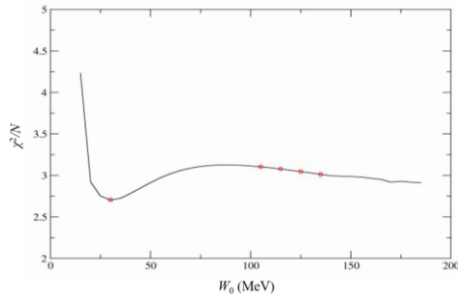


# 04 Conclusions

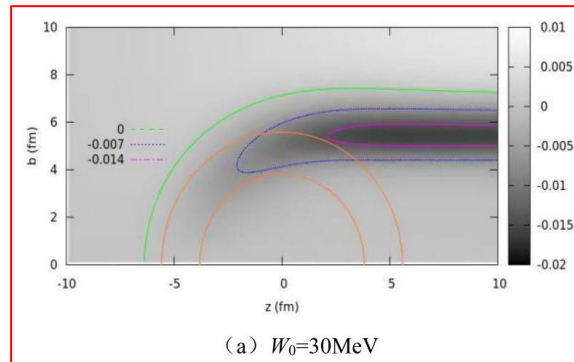
## Outlook

1. The derived **“experimental” nearside/farside components** may provide more information about nuclear potential.
2. The **semiclassical scattering method** still have many aspects needed to explore, which is helpful to unravel the physical insight of the nuclear scattering processes.

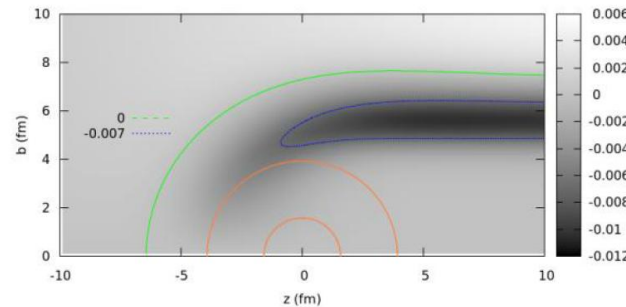
E.g., our recent preliminary work of elastic scattering quantal flux calculations, based on the Glauber model, shows its potential capability of selecting the shallow- $W$  one among the ambiguous shallow-/deep- $W$  potentials...



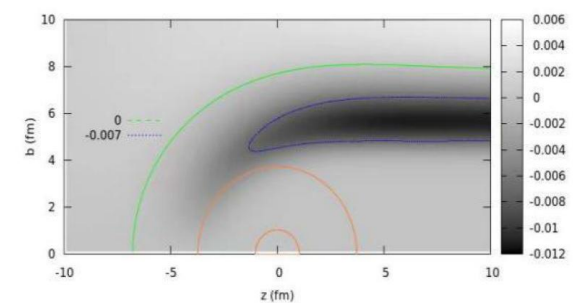
$^{12}\text{C} + ^{12}\text{C}$  at 1440 MeV



(a)  $W_0=30\text{MeV}$



(b)  $W_0=105\text{MeV}$



(c)  $W_0=115\text{MeV}$





哈爾濱工程大學  
HARBIN ENGINEERING UNIVERSITY

Thank you!

# Backup



Some details of the previous work.

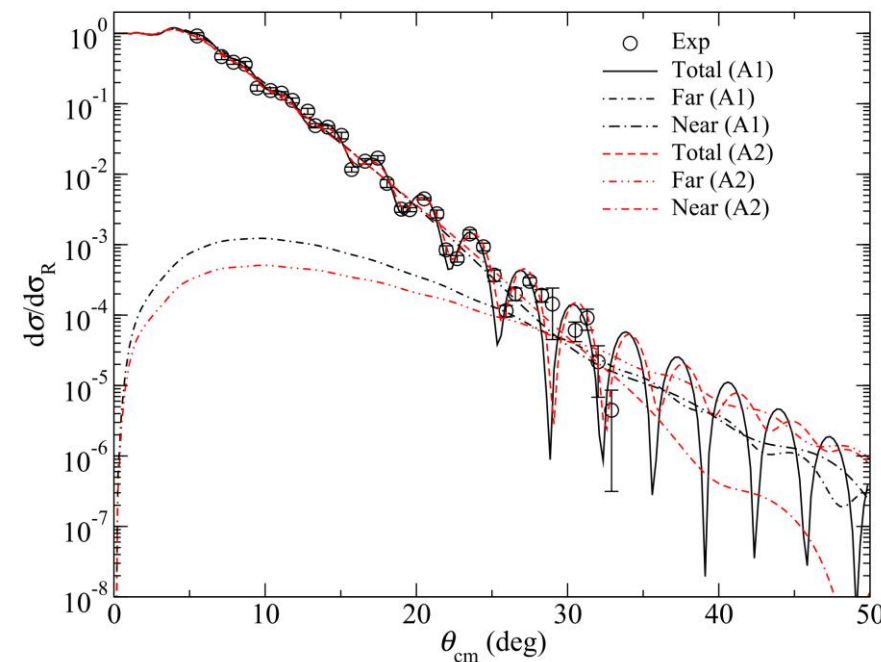
$^{16}\text{O} + ^{28}\text{Si}$  at 215.2 MeV

- OM calculation and Nearside/Farside decomposition
  - **A1: Diffractive** shallow- $V$  “E18” (also surface transparent as  $R_R > R_I$ )
  - **A2: Refractive** deep- $V$  “A-type”

| Colliding system                 | Potential set | $V_0$ (MeV) | $r_R$ (fm) | $a_R$ (fm) | $W_0$ (MeV) | $r_I$ (fm) | $a_I$ (fm) |
|----------------------------------|---------------|-------------|------------|------------|-------------|------------|------------|
| $^{16}\text{O} + ^{28}\text{Si}$ | A1            | 10.00       | 1.350      | 0.618      | 23.40       | 1.230      | 0.552      |
|                                  | A2            | 100.00      | 0.967      | 0.745      | 44.10       | 1.073      | 0.850      |

====>

- ❑ The experimental data are reproduced equally well.
- ❑ Before 35 deg, the total elastic scattering angular distributions are nearly same.
- ❑ Before 35 deg, the nearside components are close to each other, while **the farside ones are evidently different.**



# Backup



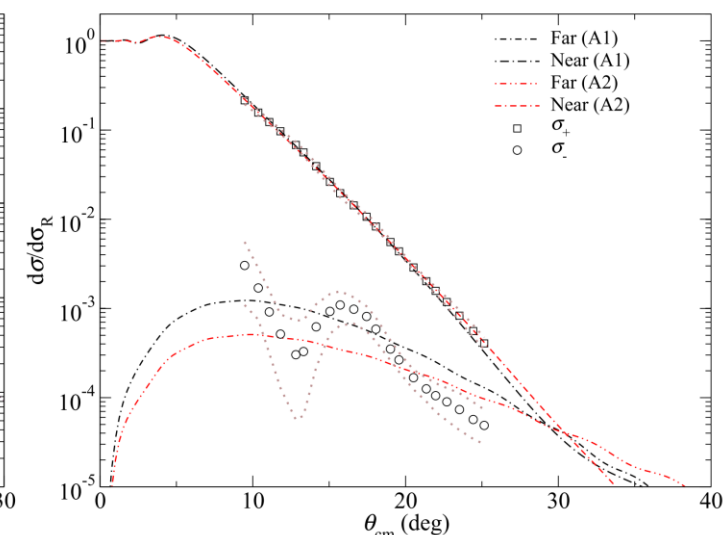
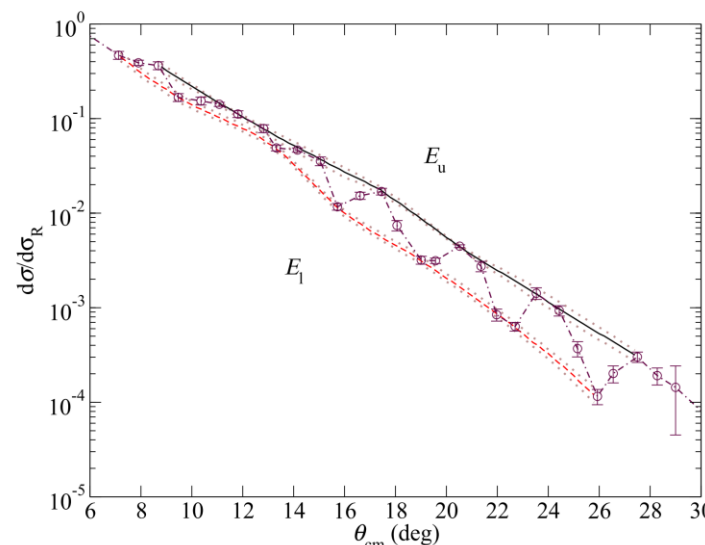
Some details of the previous work.

$^{16}\text{O} + ^{28}\text{Si}$  at 215.2 MeV

- Envelope method and comparison

===>

- $\sigma_+(\vartheta)$  and  $\sigma_n(\vartheta)$  match well.
- $\sigma_-(\vartheta)$  and  $\sigma_f(\vartheta)$  match in level of magnitude but **cannot be used to select potential in this case.**
- The difficulties encountered**
  - The **relatively small values** ( $<10^{-3}$ ) of  $\sigma_-(\vartheta)$  probably make its apparent structure meaningless.
  - The **relative error of  $\sigma_-(\vartheta)$  is significantly larger** than that of  $\sigma_+(\vartheta)$ .



# Backup



Some details of the previous work.

$^{12}\text{C} + ^{12}\text{C}$  at 1016 MeV

- OM calculation and Nearside/Farside decomposition

- B1: Surface-parent as  $R_R > R_I$

- B2: Refractive deep-V

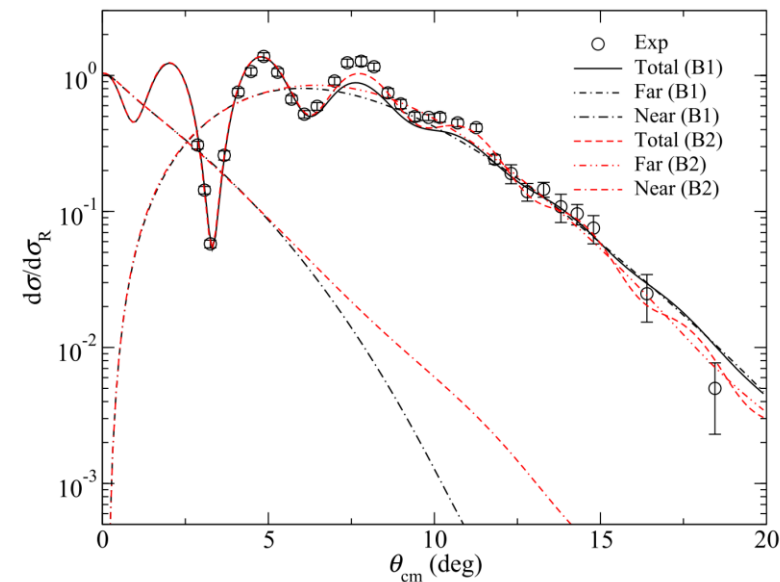
| Colliding system                | Potential set | $V_0$ (MeV) | $r_R$ (fm) | $a_R$ (fm) | $W_0$ (MeV) | $r_I$ (fm) | $a_I$ (fm) |
|---------------------------------|---------------|-------------|------------|------------|-------------|------------|------------|
| $^{12}\text{C} + ^{12}\text{C}$ | B1            | 49.90       | 0.934      | 0.742      | 150.40      | 0.262      | 1.201      |
|                                 | B2            | 129.4       | 0.681      | 0.913      | 47.90       | 0.918      | 0.622      |

[Note]

Potentials are from G.R. Satchler. Nucl. Phys. A, 505, 103-122 (1989).

==>

- ❑ The experimental data are reproduced equally well.
- ❑ The farside angular distributions are nearly same, while the nearside ones are evidently different in slope after 5 deg. (Stronger absorption of B1 potential)



# Backup



Some details of the previous work.

$^{12}\text{C} + ^{12}\text{C}$  at 1016 MeV

- Envelope method and comparison

===>

- $\sigma_-(\vartheta)$  and  $\sigma_f(\vartheta)$  match well.
- $\sigma_+(\vartheta)$  matches the  $\sigma_n(\vartheta)$  corresponding to B2 well within the limitations, selecting the potential.
- This shows the potential capability of selecting the “physical” potential among the ambiguous ones.
- This ambiguity is indeed the shallow-/deep- $W$  ambiguity.

